

# Three-body analysis reveals the significant contribution of minor ${}^5\text{He}$ $s$ -wave component in ${}^6\text{Li}(p, 2p){}^5\text{He}$ cross section

Shoya Ogawa,<sup>1,\*</sup> Kazuki Yoshida,<sup>2</sup> Yoshiki Chazono,<sup>1,3</sup> and Kazuyuki Ogata<sup>1,4</sup>

<sup>1</sup>*Department of Physics, Kyushu University, Fukuoka 819-0395, Japan*

<sup>2</sup>*Advanced Science Research Center, Japan Atomic Energy Agency, Tokai, Ibaraki 319-1195, Japan*

<sup>3</sup>*RIKEN Nishina Center for Accelerator-Based Science, 2-1 Hirosawa, Wako 351-0198, Japan*

<sup>4</sup>*Research Center for Nuclear Physics (RCNP), Osaka University, Ibaraki 567-0047, Japan*

(Dated: April 30, 2024)

**Background:**  ${}^6\text{Li}$  is usually treated as an  $\alpha + p + n$  three-body system, and the validity of this picture is important for understanding  ${}^6\text{Li}$  reactions. The  $(p, 2p)$  reaction is a powerful method to study the structure of valence nucleons in  ${}^6\text{Li}$ . Recently, the new experimental data of the  ${}^6\text{Li}(p, 2p){}^5\text{He}$  reaction have been obtained and should be analyzed.

**Purpose:** We investigate the  ${}^6\text{Li}(p, 2p){}^5\text{He}$  reaction using the  $\alpha + p + n$  three-body wave function of  ${}^6\text{Li}$  and study the validity of this model.

**Methods:** The  ${}^6\text{Li}$  wave function is used to obtain the relative wave function between  $p$  and  ${}^5\text{He}$ . We combine the relative wave function with the distorted wave impulse approximation.

**Results:** Our results reproduce the experimental data of the triple differential cross section within about 10% difference in the absolute values, and contributions from both  $p$ - and  $s$ -wave states of  ${}^5\text{He}$  in  ${}^6\text{Li}$  are found to be important.

**Conclusions:** We can qualitatively understand the  ${}^6\text{Li}(p, 2p){}^5\text{He}$  reaction by describing  ${}^6\text{Li}$  with the three-body model. Contribution from the  $s$ -wave component is important in reproducing the experimental data in the zero recoil-momentum region.

## I. INTRODUCTION

${}^6\text{Li}$  is known to have a cluster structure consisting of a deuteron ( $d$ ) and an alpha particle ( $\alpha$ ). Because of the fragileness of deuteron, nowadays,  ${}^6\text{Li}$  is described with an  $\alpha + p + n$  three-body model in many cases [1–12]. Not only static properties of  ${}^6\text{Li}$ , e.g., the binding energy and root-mean-square radius, its dynamical properties have also been studied in detail with reaction observables e.g., elastic and breakup cross sections. An interesting result was reported in Ref. [6]; the  $\alpha + d$  breakup channels play a crucial role in the elastic scattering of  ${}^6\text{Li}$ , whereas the coupling to the  $\alpha + p + n$  channels is found to be negligible. On the other hand, in the breakup reaction of  ${}^6\text{Li}$ , about one-third of the breakup cross section corresponds to the  $\alpha + p + n$  three-body channel [7]. These apparently inconsistent findings about the dynamical nature of  ${}^6\text{Li}$  should be resolved with more systematic investigation on  ${}^6\text{Li}$ . Before doing that, however, it will be meaningful to judge the three-body model for  ${}^6\text{Li}$  used in the abovementioned works [6, 7] in a different reaction, in which the single-particle (s.p.) property of the valence nucleon(s) as well as the  $\alpha + d$  clustering structure will play a crucial role.

The proton-induced proton knockout reaction,  $(p, 2p)$ , is one of the best tools to pin down the s.p. property of nuclei. In a recent review [13],  $(p, 2p)$  was shown to be an alternative to the electron-induced proton knockout reaction,  $(e, e'p)$ , which is a well-established spectroscopic tool for proton s.p. state [14, 15]. Recently, new

data of  ${}^6\text{Li}(p, 2p)$  were obtained at RCNP, Osaka University, with the double arm spectrometer with high resolution [16]. In the present work, we perform a distorted wave impulse approximation (DWIA) calculation with the  ${}^6\text{Li}$  three-body model used in Refs. [6, 7] and clarify whether the result is consistent with the  $(p, 2p)$  experimental data. In Ref. [17], a three-body description of  ${}^6\text{Li}$  was quantitatively justified by the comparison with the  $(e, e'p)$  data; the overlap function between  ${}^6\text{Li}$  and  ${}^5\text{He}$  was calculated in momentum space [4]. As mentioned in Ref. [17], the proton knockout reaction data corresponding to different energy regions of the residual nucleus  ${}^5\text{He}$  are sensitive to the  $p$ - and  $s$ -wave mixture in the ground state of  ${}^6\text{Li}$ . Therefore, a stringent test for the three-body model of Refs. [6, 7] can be done by comparing the DWIA calculation and  $(p, 2p)$  experimental data.

The construction of this paper is as follows. In Sec. II, we describe the theoretical framework. In Sec. III, we present and discuss the numerical results. Finally, in Sec. IV, we give a summary of this study.

## II. FORMALISM

### A. Gaussian expansion method

We apply the Gaussian expansion method (GEM) [18] to describe the ground state of  ${}^6\text{Li}$  and discretized-continuum states of  ${}^5\text{He}$ . In GEM, a wave function of the three-body system is expanded with the Gaussian basis on the Jacobi coordinate as shown in Fig. 1. The

\*ogawa.shoya.615@m.kyushu-u.ac.jp

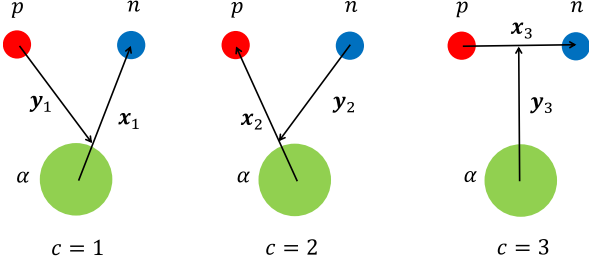


FIG. 1: Jacobi coordinate for the three-body system.

basis are described as

$$\psi_{\nu\lambda}(\mathbf{x}_c) = x_c^\lambda e^{-(x/x_\nu)^2} Y_\lambda(\Omega_{x_c}), \quad (1)$$

$$\tilde{\psi}_{\mu l}(\mathbf{y}_c) = y_c^l e^{-(y/y_\mu)^2} Y_l(\Omega_{y_c}) \quad (2)$$

with

$$x_\nu = (x_{\max}/x_0)^{(\nu-1)/\nu_{\max}}, \quad (3)$$

$$y_\mu = (y_{\max}/y_0)^{(\mu-1)/\mu_{\max}}, \quad (4)$$

where the index  $\nu$  ( $\mu$ ) means the  $\nu$ th ( $\mu$ th) basis function for the Jacobi coordinate  $\mathbf{x}_c$  ( $\mathbf{y}_c$ ), the symbol  $\lambda$  ( $l$ ) denotes the angular momentum regarding  $\mathbf{x}_c$  ( $\mathbf{y}_c$ ). Using the basis, we diagonalize the Hamiltonian:

$$h_{6\text{Li}} = K_x + K_y + V_{\alpha p} + V_{\alpha n} + V_{pn} + V_C. \quad (5)$$

Here,  $K_x$  ( $K_y$ ) means the kinetic energy operator associated with  $\mathbf{x}$  ( $\mathbf{y}$ ). The interactions for the  $p$ - $\alpha$ ,  $n$ - $\alpha$ , and  $p$ - $n$  systems are represented as  $V_{\alpha p}$ ,  $V_{\alpha n}$ , and  $V_{pn}$ , respectively, and  $V_C$  is the Coulomb interaction between  $p$  and  $\alpha$ .

The Hamiltonian of  ${}^5\text{He}$  is expressed as

$$h_{5\text{He}} = K_{x_1} + V_{\alpha n}. \quad (6)$$

Diagonalising this Hamiltonian gives a set of eigenfunctions  $\{\phi_{n\ell_B I_B M_B}\}$ , where  $n$ ,  $\ell_B$ ,  $I_B$ , and  $M_B$  are the radial quantum number, the orbital angular momentum, the total spin, and its  $z$  component, respectively, of the  $n$ - $\alpha$  system.

We introduce the overlap function defined by

$$\Psi_{n\ell_B I_B M_B M}(\mathbf{y}_1) \equiv \langle \phi_{n\ell_B I_B M_B}(\mathbf{x}_1) | \Phi_{1M}(\mathbf{x}, \mathbf{y}) \rangle_{\mathbf{x}_1}. \quad (7)$$

Here,  $\Phi_{1M}$  is the ground state wave function of  ${}^6\text{Li}$  with the total spin 1 and its  $z$  component  $M$ . The subscript  $\mathbf{x}_1$  of  $\langle \cdots \rangle$  means the integral variable. Equation (7) can be expanded as

$$\begin{aligned} \Psi_{n\ell_B I_B M_B M}(\mathbf{y}_1) &= \sum_{\ell j m m_N} (j m + m_N | I_B M_B | 1 M) \\ &\times (\ell m \frac{1}{2} m_N | j m + m_N) \varphi_{n\ell j m}(\mathbf{y}_1) \eta_{\frac{1}{2} m_N}, \end{aligned} \quad (8)$$

where  $\varphi_{n\ell j m}$  is the bound wave function of the  $p$ - ${}^5\text{He}$  system with the radial quantum number  $n$ , the orbital angular momentum  $\ell$ , its  $z$  component  $m$ , and the total spin  $j$ . The spin function of the proton is denoted by  $\eta_{\frac{1}{2} m_N}$ , where  $m_N$  is the  $z$  component of the spin.

## B. Quadruple differential cross section

We apply the DWIA to describe the  ${}^6\text{Li}(p, 2p){}^5\text{He}$  reaction. When a residual  ${}^5\text{He}$  is in the state  $\phi_{\varepsilon \ell_B I_B M_B}$  with the continuous energy  $\varepsilon$ , the transition matrix is represented as

$$T_{m_1 m_2 m_0}^{\varepsilon \ell_B I_B M_B M} = \langle \chi_{1, m_1}^{(-)} \chi_{2, m_2}^{(-)} \phi_{\varepsilon \ell_B I_B M_B} | t_{pp} | \chi_{0, m_0}^{(+)} \Phi_{1M} \rangle. \quad (9)$$

Here, the incident proton is labeled as particle 0, whereas the two emitted protons are as particle 1 and 2; the antisymmetrization between particles 1 and 2 is taken into account in  $t_{pp}$ . A distorted wave of particle  $i$  ( $i = 0, 1, 2$ ) is described as  $\chi_{i, m_i}$ , where  $m_i$  is the  $z$  component of the spin of proton. The outgoing and incoming boundary conditions of the distorted waves are denoted by superscripts (+) and (-), respectively. The  $p$ - $p$  effective interaction is denoted by  $t_{pp}$ . In this study, the spin-orbit part in each optical potential is ignored, the distorted wave is then expressed as

$$\chi_{i, m_i} = \chi_i \eta_{\frac{1}{2} m_i}, \quad (10)$$

where  $\eta_{\frac{1}{2} m_i}$  is the spin function of particle  $i$ . Inserting the complete set

$$\sum_{n \ell_B I_B M_B} |\phi_{n \ell_B I_B M_B}\rangle \langle \phi_{n \ell_B I_B M_B}| = \hat{1} \quad (11)$$

into Eq. (9), the transition matrix can be rewritten as

$$T_{m_1 m_2 m_0}^{\varepsilon \ell_B I_B M_B M} = \sum_n f_{\ell_B I_B}^n(\varepsilon) T_{m_0 m_1 m_2}^{n \ell_B I_B M_B M} \quad (12)$$

with

$$f_{\ell_B I_B}^n(\varepsilon) = \langle \phi_{\varepsilon \ell_B I_B M_B} | \phi_{n \ell_B I_B M_B} \rangle \quad (13)$$

and

$$T_{m_0 m_1 m_2}^{n \ell_B I_B M_B M} = \langle \chi_{1, m_1}^{(-)} \chi_{2, m_2}^{(-)} | t_{pp} | \chi_{0, m_0}^{(+)} \Psi_{n \ell_B I_B M_B M} \rangle. \quad (14)$$

Applying the asymptotic momentum approximation [13, 19, 20] to Eq. (14), the quadruple differential cross section (QDX) is expressed as

$$\begin{aligned} &\frac{d^4 \sigma^L}{d\varepsilon dE_1^L d\Omega_1^L d\Omega_2^L} \\ &= \sum_{\ell_B I_B} \sum_{\ell j} F_{\text{kin}} \mathcal{J}_{\text{LG}} \frac{1}{2} \frac{1}{2j+1} \left| \sum_n f_{\ell_B I_B}^n(\varepsilon) \bar{T}_{n \ell_B I_B \ell j} \right|^2. \end{aligned} \quad (15)$$

Here,  $E_1$  and  $\Omega_1$  are the energy and solid angle of particle 1, respectively, and  $\Omega_2$  is the solid angle of particle 2. The superscript L is attached to the quantities evaluated in the laboratory frame. The kinematics factor is represented as  $F_{\text{kin}}$  and  $\mathcal{J}_{\text{LG}}$  is the Jacobian from the

center-of-mass frame to the laboratory frame. The two quantities are the same as those represented in Ref. [21]. It should be noted here that the QDX is an incoherent sum of  $\ell_B$  and  $I_B$ . The reduced transition matrix is represented as

$$\bar{T}_{n\ell_B I_B \ell_j} = \sum_{m_1 m_2 m_0 m_N} \tilde{t}_{m_1 m_2 m_0 m_N} \int d\mathbf{R} \chi_1^{(-)*}(\mathbf{R}) \chi_2^{(-)*}(\mathbf{R}) \chi_0(\mathbf{R}) e^{i\mathbf{K}_0 \cdot \mathbf{R}/A} \sum_m (\ell m \frac{1}{2} m_N | j m + m_N) \varphi_{n\ell j m}(\mathbf{R}), \quad (16)$$

where  $\mathbf{R}$  is the relative coordinate between  ${}^5\text{He}$  and each particle,  $\mathbf{K}_0$  is the wavenumber of the incident proton, and  $A$  is the mass number of  ${}^6\text{Li}$ . The transition matrix of the elementary process is written as

$$\tilde{t}_{m_1 m_2 m_0 m_N} = \langle \eta_{\frac{1}{2}m_1} \eta_{\frac{1}{2}m_2} e^{i\boldsymbol{\kappa}' \cdot \mathbf{s}} | t_{pp}(\mathbf{s}) | \eta_{\frac{1}{2}m_0} \eta_{\frac{1}{2}m_N} e^{i\boldsymbol{\kappa} \cdot \mathbf{s}} \rangle. \quad (17)$$

Here  $\mathbf{s}$  is the relative coordinate between the two protons and  $\boldsymbol{\kappa}$  ( $\boldsymbol{\kappa}'$ ) is the relative wavenumber between the two protons in the initial (final) state. Equation (16) is calculated by using a code PIKOE [21].

We calculate the following triple differential cross section (TDX) for comparison with the experimental data:

$$\frac{d^3\sigma^L}{dE_1^L d\Omega_1^L d\Omega_2^L} = \int_{\varepsilon_{\min}}^{\varepsilon_{\max}} d\varepsilon \frac{d^4\sigma^L}{d\varepsilon dE_1^L d\Omega_1^L d\Omega_2^L}. \quad (18)$$

The interval of integration ( $\varepsilon_{\min}$ ,  $\varepsilon_{\max}$ ) is determined according to the experimental data.

### III. RESULTS AND DISCUSSION

#### A. The ground state of ${}^6\text{Li}$

In this study, we take the Minnesota interaction [22] and the KKNN potential [23] for the  $p$ - $n$  and the nucleon- $\alpha$  interactions, respectively, in the calculation of the ground state of  ${}^6\text{Li}$  with GEM. To reproduce the binding energy of  ${}^6\text{Li}$ , a phenomenological three-body interaction

$$V_{3b}(x, y) = V_3 e^{-\gamma(x^2 + y^2)} \quad (19)$$

is added to  $h_6\text{Li}$ ; we adopt  $V_3 = -0.4$  MeV and  $\gamma = 0.036 \text{ fm}^{-2}$ . The parameter sets of the Gaussian basis are summarized in Table I. The results of the ground-state energy and root-mean-square radius are shown in Table II, which reproduce well the experimental data [24, 25].

We calculate  ${}^5\text{He}$  energy distribution for individual spin-parity state in the ground state of  ${}^6\text{Li}$ :

$$P(\varepsilon) = \sum_{M_B} \int d\mathbf{y}_1 \left| \sum_n f_{\ell_B I_B}^n(\varepsilon) \Psi_{n\ell_B I_B M_B}(\mathbf{y}_1) \right|^2. \quad (20)$$

TABLE I: Parameters of Gaussian basis

c	$i_{\max}$	$x_0$ [fm]	$x_{\max}$ [fm]	$j_{\max}$	$y_0$ [fm]	$y_{\max}$ [fm]
1, 2	10	0.5	12.0	10	0.5	12.0
3	10	0.1	12.0	10	0.5	12.0

TABLE II: The ground-state energy and root-mean-square radius of  ${}^6\text{Li}$ . The experimental data are taken from Refs. [24, 25].

Cal.		Exp.	
$\varepsilon_0$ [MeV]	$r_{\text{rms}}$ [fm]	$\varepsilon_0$ [MeV]	$r_{\text{rms}}$ [fm]
-3.77	2.36	-3.6989	2.44 $\pm$ 0.07

We show the value of  $P = \int P(\varepsilon) d\varepsilon$  for the  $p$ - and  $s$ -wave states of  ${}^5\text{He}$  in Table III. The contributions of higher angular momentum states are found to be negligibly small and not considered in the following discussion. The  $p$ -wave states of  ${}^5\text{He}$  are found to be dominant in  ${}^6\text{Li}$ . We also show the energy distribution of the probability in Fig. 2. The solid, dotted, and dashed lines represent  $P(\varepsilon)$  of  ${}^5\text{He}(p_{3/2})$ ,  ${}^5\text{He}(p_{1/2})$ , and  ${}^5\text{He}(s_{1/2})$ , respectively. The probability of  ${}^5\text{He}(p_{3/2})$  and  ${}^5\text{He}(p_{1/2})$  have peak structures around 0.8 MeV and 3 MeV, respectively, which are near the resonant energies of the narrow and broad resonances [26], respectively. It indicates that these  ${}^5\text{He}$  resonances exist in  ${}^6\text{Li}$ . On the other hand, the absolute value of  $P(\varepsilon)$  for  ${}^5\text{He}(s_{1/2})$  is very small. However, as shown in Sec. III B, this state makes a significant contribution to the TDX.

TABLE III:  ${}^5\text{He}$  probability of each state in the ground state of  ${}^6\text{Li}$ .

	${}^5\text{He}(s_{1/2})$	${}^5\text{He}(p_{3/2})$	${}^5\text{He}(p_{1/2})$
$P$	0.102	0.551	0.275

#### B. ${}^6\text{Li}(p, 2p){}^5\text{He}$ reaction

We analyze the  ${}^6\text{Li}(p, 2p){}^5\text{He}$  reaction at 392 MeV. The polar and azimuthal angles of the particle 1 (2) in the fi-

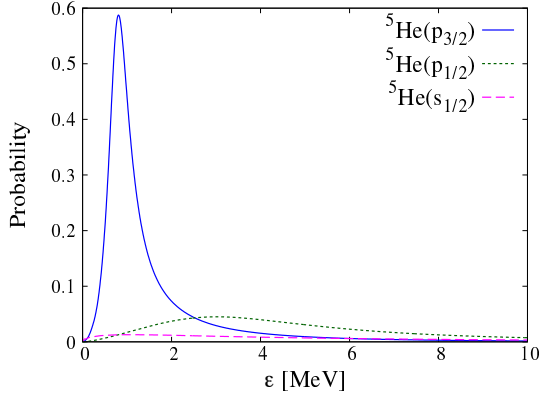


FIG. 2: Energy distribution of each  ${}^5\text{He}$  state in  ${}^6\text{Li}$ .

nal state are fixed at  $32.21^\circ$  and  $0^\circ$  ( $51.62^\circ$  and  $180^\circ$ ), respectively. We use the Franey-Love effective interaction for  $t_{pp}$  [27]. The optical potentials of the  $p$ - ${}^6\text{Li}$  and  $p$ - ${}^5\text{He}$  systems are constructed by folding the Melbourne  $g$  matrix [28, 29] with the densities of  ${}^6\text{Li}$  and  ${}^5\text{He}$ , respectively. The densities are obtained by using GEM. The Coulomb potentials are constructed by assuming a uniformly charged sphere as shown in Ref. [30]. In the present analysis, we investigate the reactions where  $p_{3/2}$ ,  $p_{1/2}$ , and  $s_{1/2}$  valence protons are knocked out.

The QDXs leaving  ${}^5\text{He}(p_{3/2})$ ,  ${}^5\text{He}(p_{1/2})$ , and  ${}^5\text{He}(s_{1/2})$  residues are shown in Fig. 3 as functions of  $\varepsilon$  and the kinetic energy  $T_1^L$  of particle 1. For the  $T_1^L$  distribution, one can see the typical single- and double-peaked shapes of  $s$ - and  $p$ -wave nucleon knock-outs, respectively. The QDXs for  ${}^5\text{He}(p_{3/2})$  and  ${}^5\text{He}(p_{1/2})$  have peak structures at the resonant energies with respect to  $\varepsilon$ . The absolute value of QDX for  ${}^5\text{He}(s_{1/2})$  is larger than that for  ${}^5\text{He}(p_{1/2})$  even though  ${}^5\text{He}(s_{1/2})$  has much lower  $P$  in  ${}^6\text{Li}$ . This can be understood from the difference in the maximum values of the Fourier transform of  $\varphi_{nljm}$ . In fact, when an  $s$ -wave proton is knocked out from  ${}^{40}\text{Ca}$ , the TDX tends to have a large absolute value, as seen in Fig. 21 of Ref. [13]. This is because the momentum distribution of the  $s$ -wave nucleon is well localized around the zero momentum and its peak height can be larger than that for the  $p$ -waves, even though the integrated value of the former is significantly smaller than that of the latter.

Finally, we show the TDX calculated by using Eq. (18) with  $(\varepsilon_{\min}, \varepsilon_{\max}) = (0.4, 1.8)$  and  $(0.4, 14.8)$  by the thick lines in Figs. 4 and 5, respectively. The dotted, dashed, and dot-dashed lines correspond to the results when the residues are  ${}^5\text{He}(p_{3/2})$ ,  ${}^5\text{He}(p_{1/2})$ , and  ${}^5\text{He}(s_{1/2})$ , respectively. Our results reproduce the shapes of the experimental data [16] well, but slightly overshoot the absolute values; we also show the TDXs multiplied by a normalization factor by the thin solid line. Possible origin of this overshooting is that the breakup of  ${}^5\text{He}$  in the propagation in the exit channel is not taken into account in the present analysis. Another possibility will be the systematic error of the experimental data, which is esti-

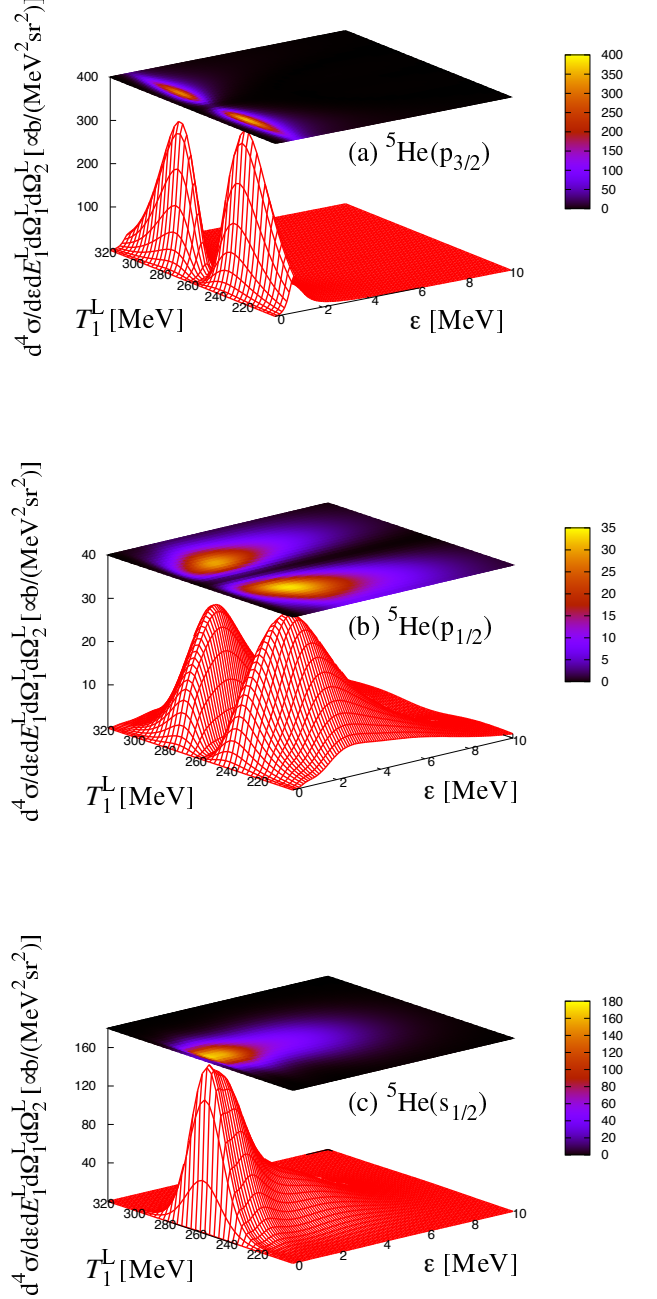


FIG. 3: QDXs of  ${}^6\text{Li}(p, 2p){}^5\text{He}$  leaving (a)  ${}^5\text{He}(p_{3/2})$ , (b)  ${}^5\text{He}(p_{1/2})$ , and (c)  ${}^5\text{He}(s_{1/2})$  residue.

mated about 10% [31]. In the results for the two energy ranges, the contributions of  ${}^5\text{He}(s_{1/2})$  to the TDXs at  $T_1^L \sim 260$  MeV are significant and fill the dips in the total TDXs. The  ${}^5\text{He}(s_{1/2})$  contribution becomes more important when we see the TDX corresponding to higher  $\varepsilon$ . The fact that our calculation reproduces well the TDXs for both  $\varepsilon$  regions indicates that the proton s.p. nature

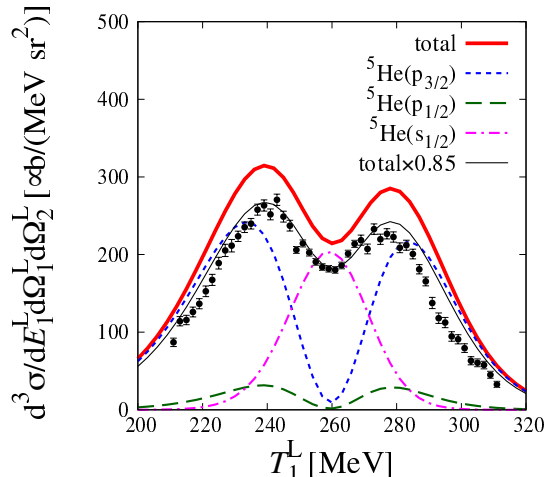


FIG. 4: TDX calculated by using Eq. (18) with  $(\epsilon_{\min}, \epsilon_{\max}) = (0.4, 1.8)$ . The experimental data are taken from Ref. [16]

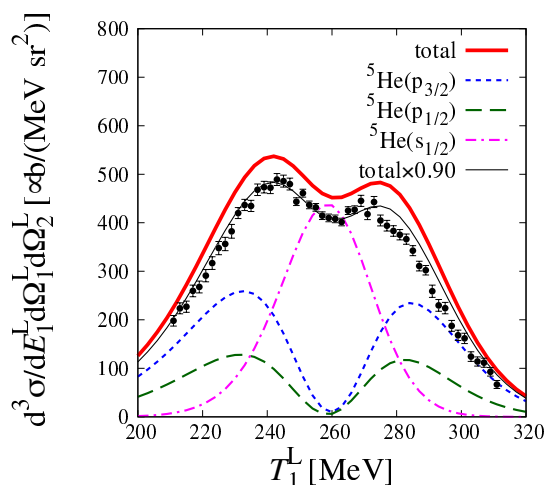


FIG. 5: Same as in Fig. 4 but for  $(\epsilon_{\min}, \epsilon_{\max}) = (0.4, 14.8)$ .

of  ${}^6\text{Li}$  is properly described with the three-body model adopted. It should be noted that in the setup of the  ${}^6\text{Li}(p,2p)$  experiment, the finite-size effect of the detectors, which usually affect the TDX around the dip, was minimized [16]. We also have confirmed this.

#### IV. SUMMARY

We analyzed the  ${}^6\text{Li}(p,2p){}^5\text{He}$  reaction by using DWIA and the three-body model. The  $p$ -wave states of  ${}^5\text{He}$  dominate in  ${}^6\text{Li}$ , while the probability of the  $s$ -wave state is about 10%. In TDX analysis, both  $p$ - and  $s$ -wave contributions are important, and in particular, the dip in the experimental data is reproduced by the  ${}^5\text{He}(s_{1/2})$  component. Our results reproduce the experimental data of the TDX within about 10% difference in the absolute values. These results indicate that we can qualitatively describe the s.p. property of  ${}^6\text{Li}$ , which is consistent with the  ${}^6\text{Li}(p,2p){}^5\text{He}$  reaction data by using an  $\alpha + p + n$  three-body model. As a next step, the  $\alpha + d$  structure of  ${}^6\text{Li}$  should be judged. For this purpose, we will analyze the  ${}^6\text{Li}(p,pd)\alpha$  reaction by combining the three-body model with CDCCIA [32], which is a new reaction model to describe the reaction for knocking out a weakly bound cluster.

#### Acknowledgments

The authors thank H. P. Yoshida and T. Noro for providing them with the experimental data. S.O. and K.O. thank T. Wakasa for helpful discussions. This work is supported in part by Grant-in-Aid for Scientific Research (No. JP20K14475, and No. JP21H04975) from Japan Society for the Promotion of Science (JSPS) and JST ER-ATO Grant No. JPMJER2304, Japan.

- 
- [1] V. Kukulín, V. Voronchev, T. Kaipov, and R. Er-amzhyan, Nucl. Phys. A **517**, 221 (1990).
  - [2] L. Hlophe, J. Lei, C. Elster, A. Nogga, and F. M. Nunes, Phys. Rev. C **96**, 064003 (2017).
  - [3] E. M. Tursunov, A. S. Kadyrov, S. A. Turakulov, and I. Bray, Phys. Rev. C **94**, 015801 (2016).
  - [4] C. T. Christou, D. R. Lehman, and W. C. Parke, Phys. Rev. C **37**, 445 (1988).
  - [5] Y. Kikuchi, N. Kurihara, A. Wano, K. Katō, T. Myo, and M. Takashina, Phys. Rev. C **84**, 064610 (2011).
  - [6] S. Watanabe, T. Matsumoto, K. Ogata, and M. Yahiro, Phys. Rev. C **92**, 044611 (2015).
  - [7] S. Watanabe, K. Ogata, and T. Matsumoto, Phys. Rev. C **103**, L031601 (2021).
  - [8] J. Bang and C. Gignoux, Nucl. Phys. A **313**, 119 (1979).
  - [9] D. R. Lehman and M. Rajan, Phys. Rev. C **25**, 2743 (1982).
  - [10] D. R. Lehman and W. C. Parke, Phys. Rev. C **28**, 364 (1983).
  - [11] A. Cs6t6 and R. G. Lovas, Phys. Rev. C **46**, 576 (1992).
  - [12] N. Yamanaka and E. Hiyama, Phys. Rev. C **91**, 054005 (2015).
  - [13] T. Wakasa, K. Ogata, and T. Noro, Prog. Part. Nucl. Phys. **96**, 32 (2017).
  - [14] J. J. Kelly, in *Advances in Nuclear Physics*, edited by J. W. Negele and E. Vogt, vol. 23, p. 75 (Plenum Press, New York, 1996).
  - [15] G. Kramer, H. Blok, and L. Lapik6s, Nucl. Phys. A **679**,



- 267 (2001).
- [16] H. P. Yoshida, Ph.D. thesis, Kyushu University (2010).
  - [17] J. B. J. M. Lanen, A. M. van den Berg, H. P. Blok, J. F. J. van den Brand, C. T. Christou, R. Ent, A. G. M. van Hees, E. Jans, G. J. Kramer, L. Lapikás, et al., Phys. Rev. Lett. **62**, 2925 (1989).
  - [18] E. Hiyama, Y. Kino, and M. Kamimura, Prog. Part. Nucl. Phys. **51**, 223 (2003).
  - [19] K. Yoshida, K. Minomo, and K. Ogata, Phys. Rev. C **94**, 044604 (2016).
  - [20] K. Yoshida, Y. Chazono, and K. Ogata, arXiv:2404.04115 (2024).
  - [21] K. Ogata, K. Yoshida, and Y. Chazono, Comput. Phys. Commun. **297**, 109058 (2024).
  - [22] D. Thompson, M. Lemere, and Y. Tang, Nucl. Phys. A **286**, 53 (1977).
  - [23] H. Kanada, T. Kaneko, S. Nagata, and M. Nomoto, Prog. Theor. Phys. **61**, 1327 (1979).
  - [24] D. Tilley, C. Cheves, J. Godwin, G. Hale, H. Hofmann, J. Kelley, C. Sheu, and H. Weller, Nucl. Phys. A **708**, 3 (2002).
  - [25] A. Dobrovolsky, G. Alkhazov, M. Andronenko, A. Bauchet, P. Egelhof, S. Fritz, H. Geissel, C. Gross, A. Khanzadeev, G. Korolev, et al., Nucl. Phys. A **766**, 1 (2006).
  - [26] F. Ajzenberg-Selove and T. Lauritsen, Nucl. Phys. A **227**, 1 (1974).
  - [27] M. A. Franey and W. G. Love, Phys. Rev. C **31**, 488 (1985).
  - [28] K. Amos, P. J. Dortmans, H. V. von Geramb, S. Karataglidis, and J. Raynnal, in *Advances in Nuclear Physics*, edited by J. W. Negele and E. Vogt, p. 276 (Springer US, Boston, MA, 2000).
  - [29] K. Minomo, K. Ogata, M. Kohno, Y. R. Shimizu, and M. Yahiro, J. Phys. G **37**, 085011 (2010).
  - [30] A. Koning and J. Delaroche, Nucl. Phys. A **713**, 231 (2003).
  - [31] T. Wakasa, private communication (2023).
  - [32] Y. Chazono, K. Yoshida, and K. Ogata, Phys. Rev. C **106**, 064613 (2022).